Theoretical Study of Determination the Energy Gap of Murrastanine-A Conjugated Metal Using Density Functional Theory (DFT)

Alvira Rahmadani Putri[1], I Gusti Made Sanjaya[2]

[1,2]Department of Chemistry, Faculty of Mathematics and Natural Sciences, Universitas Negeri Surabaya, Indonesia

ABSTRACT: The research has been carried out to determine the energy gap of the compound murrastanine-a conjugated with period 4 metals. The calculation of the energy gap is carried out theoretically using computational methods with density functional theory (DFT) and the basis set 6-31G*/B3LYP through NWChem software. The results showed that all period 4 metal conjugations could reduce the energy gap of the murrastanine-a compound except for conjugation with gallium metal. The energy gap of the murrastanine-a compound decreased from 4.479 eV to 4.444 until 0.019 eV. The presence of conjugation with metals makes the energy gap of murrastanine-a diverse so that it can increase its potential use. CaM_2, CuM_2, and AsM_5 complexes can be potential as high-temperature sensors. CrM_6 and FeM_2 complexes can be potential as solar cells. KM, CaM_2, TiM4, ZnM_2, GeM_2, and AsM_3 complexes can be potential as blue LED devices. Complex compounds resulting from the conjugation process with period 4 metals can be formed stably except for complexes with potassium and calcium metals which are characterized by the absence of charge distribution.

KEYWORDS: DFT, Energy gap, Murrastanine-a, Organic semiconductor, Period 4 metals.

INTRODUCTION

Currently, the application of organic compounds is increasingly being carried out, including as organic semiconductor materials in the manufacture of sensors. Semiconductors are materials that can behave as conductors or insulators at certain times because semiconductors have an energy gap between the conductor and insulator material [1]. In general, the semiconductor energy gap is in the range of 0.2 to 2 eV [2].

In semiconductor materials, there can be excitation of electrons towards the conduction band caused by several external influences such as light and temperature [3]. When the conduction band is filled, the material behaves as a conductor, and when the conduction band is not filled with electrons, the material behaves as an insulator [4]. Materials with an energy gap of 1.12 to 3.2 eV can be applied as high-temperature sensors with a range of 20 to 600 °C [5], [6]. Body temperature sensors that are widely used at this time are non-contact sensors that use infrared sensors [6], materials that meet the infrared spectra have an energy gap ranging from 0 to 1.5 eV [7]. As for the use of semiconductors related to the influence of light, it has been widely applied as solar cell devices using materials with an energy gap between 0.93 to 1.61 eV [8]. For light converter devices that can work indoors, namely indoor photovoltaic which can work optimally using materials that have an energy gap of 1.80 to 1.90 eV [9], [10]. In addition, some semiconductors can be affected by electric currents and emit light, namely light-emitting diodes (LEDs), there are several types of LEDs, one of which is blue LEDs which use materials with an energy gap of 2.7 to 4.2 eV [11].

Organic compounds that have the potential as semiconductor materials are organic compounds that have conjugated double bonds. The presence of conjugated double bonds allows the process of absorption of electromagnetic waves so that electrons can be excited from the ground level to the excitation level [12]. In general, organic semiconductor compounds have a larger energy gap than inorganic semiconductors, that is 2 to 3 eV, with a large energy gap making the sensitivity of organic semiconductors not as good as inorganic semiconductors. Several things can be done to reduce the energy gap, one of which is by making organic complexes which are a combination of materials with high electron affinity (electron acceptors) and compounds with low ionization energies (electron donors). The transfer of charge between the molecules of the material can increase the conductivity of the material [13].

One of the organic compounds that have properties as a semiconductor is the murrastanine-a compound. Murrastanine-a compounds can be found in the bay koja plant which has the Latin name *Murraya keonigii*. The compound murrastanine-a was isolated from the methanol extract of the bark as a brownish-colored oil [14]. Murrastanine-a is a carbazole derivative in which

carbazole is an organic semiconductor compound that has been successfully applied as an OLED material with an energy gap of 3.5 eV [15].

To reduce the energy gap of the compound murrastanine-a, in this study, conjugation was carried out with period 4 metals, that is from potassium metal to arsenic, which these metals can form complex compounds [16]–[20]. The energy gap is determined from the difference between the HOMO energy and the LUMO energy. The energy gap value indicates the electrical conduction of both the semiconductor and the insulator [21].

In this study, the energy values of HOMO and LUMO were calculated theoretically using a computational method with density functional theory (DFT) and a basis set of 6-31G*/B3LYP. The basis of the DFT method is the calculation of electronic energy determined from the electron density (ρ). In other words, there is a one-to-one correspondence between the density of a system and the energy. The purpose of the DFT method is to design a function that relates electron density to energy [22]. In modern DFT there are several functions designed to find an accurate and computationally feasible approach, one of which is a hybrid function in which some of the exact exchange fraction (HF) is calculated using Kohn-Sham (KS) orbitals. The B3LYP function belongs to the hybrid function category, which is one of the most used functions in DFT applications [23]. B3LYP can be called a hybrid function because it is the result of the combination of the Hartree-Fock estimate with energy exchange and the DFT estimate with energy exchange, all of which are combined in a function that includes electron correlation [22].

The basis set used in this study is 6-31G* which belongs to the polarized base set. On a polarized basis set, the angular momentum function is added to the function describing the atomic orbitals [24]. This basis set is used to describe the density polarization of other atomic fields. Since only electrons in the valence orbitals are polarized to some degree, the polarization function is included only for valence electrons [25].

The use of the DFT method with the B3LYP function and the basis set 6-31G* has been successfully carried out for the calculation of the energy of the HOMO and LUMO bands in organic semiconductors as has been done by Pamungkas and Sanjaya, 2013 in determining the energy gap of calcium metal conjugated porphyrin compounds [12], as well as by Wahyudah, 2016 in determining the energy gap of delphinidin complex compounds [4].

MATERIALS AND METHODS
Hardware and Software
Calculations were carried out using a computer with specifications: Intel Xeon, CPU E5-2609 v4 1.70GHz with Ubuntu 20.04.1 operating system. The software used in this research are: Avogadro, NWChem, and Jmol. Avogadro was used for the initial modeling of the structure of the murrastanine-a complex with metal and creating the input file for the calculation of the energy gap, NWChem was used for computational calculation of the energy gap of the complex compound murrastanine-a with metal, and Jmol was used to visualize the electron distribution of the murrastanine-a complex with metal.

Methods
Initial Modeling
The structure of murrastanine-a compounds and murrastanine-a complexes with period 4 metals was drawn using Avogadro software, and the structure of metal complexes with murrastanine-a was adjusted to the oxidation state of the metal. After that, to minimize the structure, geometry optimization is carried out, then the file is saved as a PDB file.
Energy Gap Calculation
From the compound structure file that has been created, then an input file is created for the calculation of the HOMO and LUMO energy bands on the NWChem software using the Avogadro software. In making the input file, the calculation method, basis set, compound charge, and multiplicity adjustment are selected. This study used single point energy calculation with the DFT method and basis set 6-31G*/B3LYP. Then the input file is saved as file.nw which is then used in the calculation of the energy of the HOMO and LUMO bands. The calculation steps in the NWChem software are carried out according to the method described by Valiev et al, 2010 in the article "NWChem: A comprehensive and scalable open-source solution for large-scale molecular simulations" [26]. The results of the calculations on the NWChem software are in the form of a log file containing energy data including energy data for the HOMO and LUMO bands, then the energy gap of the compound is determined from the calculation of the difference between the energy of the HOMO and LUMO bands.

Visualization of Charge Distribution

The charge distribution of murrastanine-a complexes with metal was visualized using Jmol. The log file calculated from NWChem is opened with Jmol, then the surface menu is selected, and then the molecular electrostatic potential is selected to display the distribution of electrons from metal complex compounds with murrastanine-a.

RESULTS AND DISCUSSION

Results of Modeling the Structure of Murrastanine-a with its Metal Complex

The modeling of the murrastanine-a structure was carried out using Avogadro. The structure of the murrastanine-a compound is shown in the figure below:
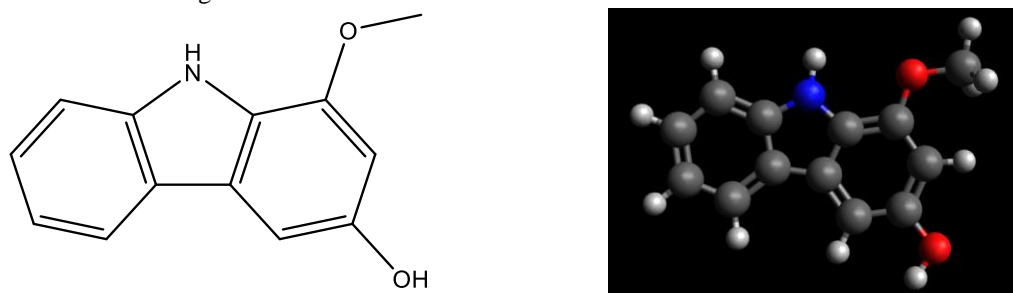

Figure 1. Structure of murrastanine-a compound

Modeling of murrastanine-a metal complex (MMu) was also carried out using Avogadro software. The metals used are all metals in period 4, from potassium to arsenic. The complex structure is adapted to the oxidation state of each metal.
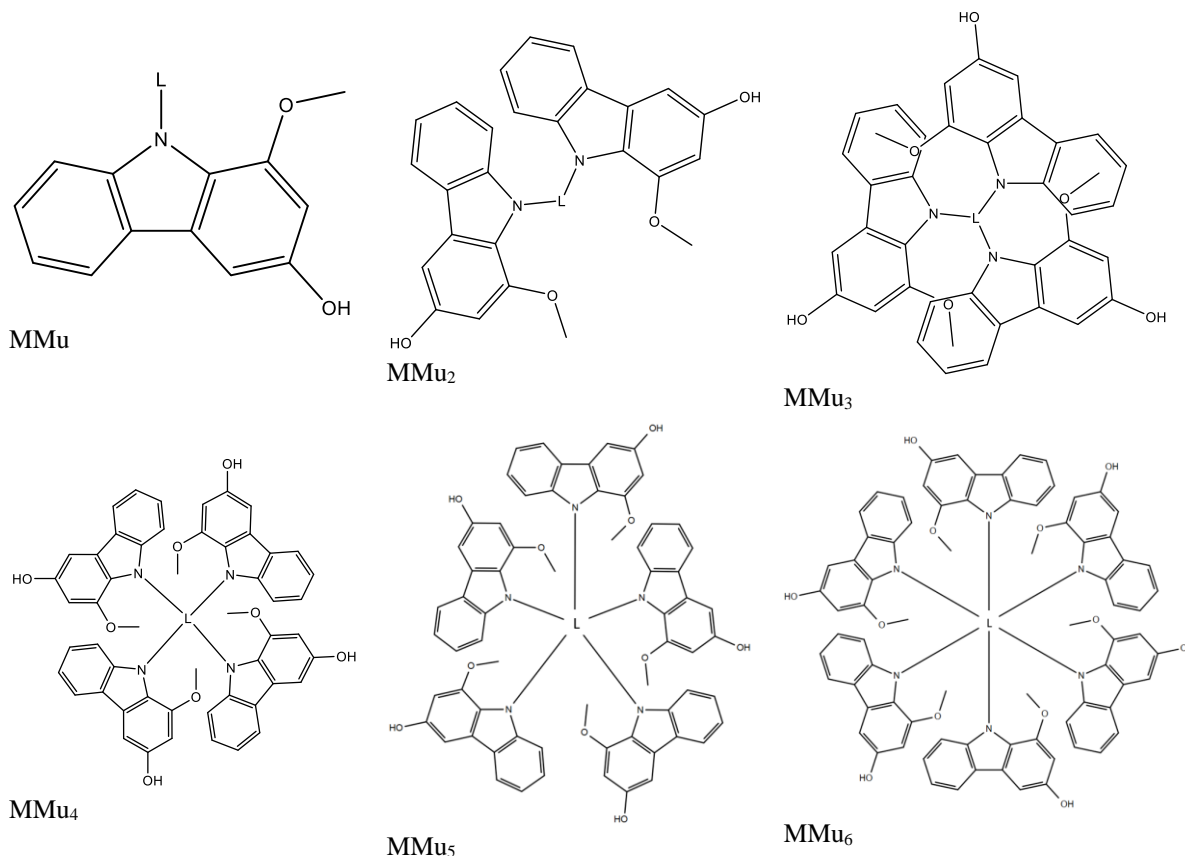

Figure 2. The structure of murrastanine-a metal complex

In this research, the main oxidation state of each metal is used. The metal will be the central atom and bonded to the nitrogen atom of the murrastanine-a compound. The tendency of the bonds formed is coordination bonds caused by the presence of empty orbitals on metal atoms so that they can be occupied by electrons owned by nitrogen in murrastanine-a. After modeling, the metal structure with murrastanine-a was optimized to obtain a stable structure with a minimum energy level.

Results of the Energy Gap Murrastanine-a Complex

The energy gap is calculated from the difference between the energy of HOMO and LUMO. The energy values for HOMO and LUMO are obtained from the single-point energy calculation using the DFT method by NWChem software. The results of the energy gap calculation are shown in the following table:

Table 1. The result of the energy gap calculation

No.	Compound	Homo (Hartree)	Lumo (Hartree)	Eg (Hartree)	Eg (Ev)
1	Murrastanine-A	-0.182985	-0.018366	0.164619	4.479513457
2	KM	-0.183583	-0.039400	0.144183	3.923421286
3	CaM_2	-0.185292	-0.084022	0.101270	2.755698478
4	ScM_3	-0.187235	-0.023906	0.163329	4.444410751
5	TiM_4	-0.182425	-0.026344	0.156081	4.247182523
6	VM_5	-0.165281	-0.146591	0.018690	0.508581066
7	CrM_3	-0.073564	-0.072865	0.000699	0.019020769
8	CrM_6	-0.151448	-0.115445	0.036003	0.979692034
9	MnM_4	-0.153462	-0.152016	0.001446	0.039347684
10	MnM_2	-0.142856	-0.141874	0.000982	0.026721595
11	FeM_2	-0.222449	-0.184536	0.037913	1.031665808
12	FeM_3	-0.183736	-0.159722	0.024014	0.653454560
13	CoM_3	-0.183361	-0.178529	0.004832	0.131485485
14	CoM_2	-0.186846	-0.178576	0.008270	0.225038278
15	NiM_2	-0.187581	-0.181105	0.006476	0.176221026
16	CuM	-0.182578	-0.160659	0.021919	0.596446677
17	CuM_2	-0.180299	-0.083444	0.096855	2.635560147
18	ZnM_2	-0.183368	-0.058686	0.124682	3.392771775
19	GaM_3	-0.185361	-0.020430	0.164931	4.488003413
20	GeM_4	-0.181897	-0.024598	0.157299	4.280326009
21	GeM_2	-0.185142	-0.047184	0.137958	3.754030321
22	AsM_5	-0.171162	-0.095711	0.075451	2.053127341
23	AsM_3	-0.177048	-0.021701	0.155347	4.227209356

The results of the energy gap of murrastanine-a compounds after conjugation with period 4 metals are known to have succeeded in producing complex compounds with lower energy gaps than the energy gap of murrastanine-a compounds before being conjugated with metals, except in conjugation with gallium metal which produces complex compounds with a higher energy gap value than the initial energy gap of murrastanine-a compounds. Following research conducted by Khorsand Zak et al, 2016 who reported that the addition of gallium dopants to ZnO compounds could increase the value of the energy gap [27], and research conducted by Narayanan et al, 2018 which reported that the energy gap of $Zn_{0.85}Ca_{0.15}O$ increased after the addition of gallium dopants, and the energy gap continued to increase with the increase in the concentration of gallium dopant, this could occur due to

the Burstein-Moss effect [28]. The Burstein-Moss effect is related to changes in the state of electronic energy levels in the conduction band and valence band of semiconductor materials that are given impurities of other elements [29].

From the results of conjugation with period 4 metals, it is known to have produced complex compounds with various energy gaps. The resulting drop in energy gap ranges from 4.444 to 0.019 eV.

Table 2. Potential uses of the murrastanine-a complexes

Kompleks LM	Celah Energi	Potensi Kegunaan
VM_5, CrM_3, CrM_6, MnM_4, MnM_2, FeM_2, FeM_3, CoM_2, CoM_3, NiM_2, CuM	0,019 – 1,031 eV	Sensor inframerah, sensor suhu tubuh
CaM_2, CuM_2, AsM_5	2,053 – 2,756 eV	Sensor suhu tinggi
CrM_6 dan FeM_2	0,979 – 1,031 eV	Sel Surya
KM, CaM_2, TiM_4, ZnM_2, GeM_2, AsM_3	2,756 – 4,247 eV	*Blue* LED

The diversity of energy gaps resulting from metal conjugation makes the potential use of murrastanine-a compounds as organic semiconductors to be wider in several fields, such as temperature sensors, light sensors, solar cells, and LED devices.

Results of Murrastanine-a and Murrastanine-a Complexes Predicted Stability Visualization

The stability of murrastanine-a metal complex can be seen from the charge distribution on the complex in addition to its symmetry and dipole moment. Stable complexes are caused by the ability of the ligands to coordinate the central atom and the magnitude of the charge on the metal which makes the electrostatic attraction with the metal stronger, resulting in a dense complex [4], [12], in the presence of a dense complex so that the distribution of charge between the central metal and the compound murrastanine-a can occur.

The charge distribution can be described by visualizing the electrostatic potential surface (ESP) which can show the probability of the presence of electrons in Cartesian coordinates (x, y, z) in a molecule. **Figure 3a** shows the color scheme of the ESP, the red one indicates the negative area while the blue one shows the positive region.
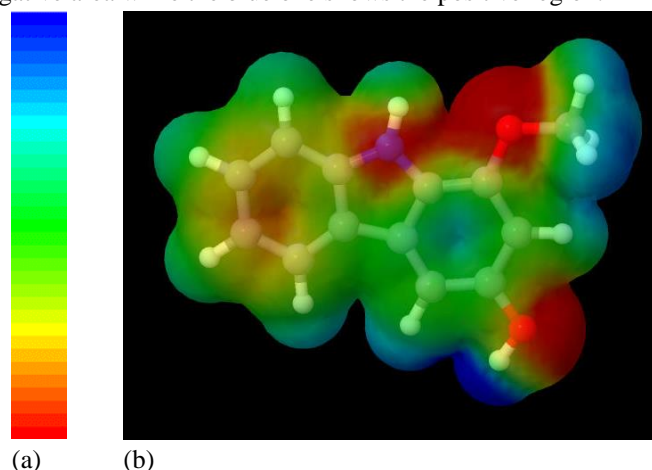

(a)   (b)

Figure 3. (a) ESP color scheme, (b) ESP visualization of murrastanine-a in Jmol

Generally, ligands have more electronegative atoms, so they can donate electron pairs to the central metal cation to form coordination covalent [30]. The visualization of the electron distribution of the compound murrastanine-a **(figure 3b)**, shows that the nitrogen atom is a negative area where the metal will bind to that part. When the metal is bound to the compound murrastanine-a, there can be a charge distribution. The charge distribution occurs as a result of the combination of a molecule with an electron donor group and a molecule with an electron-accepting group [31]. The occurrence of a charge distribution marked in the center of the complex will tend to form a neutral region, whereas if there is no charge distribution, the central metal remains a positive region marked in blue. Following are the results of the visualization of metal complex ESP with murrastanine-a:
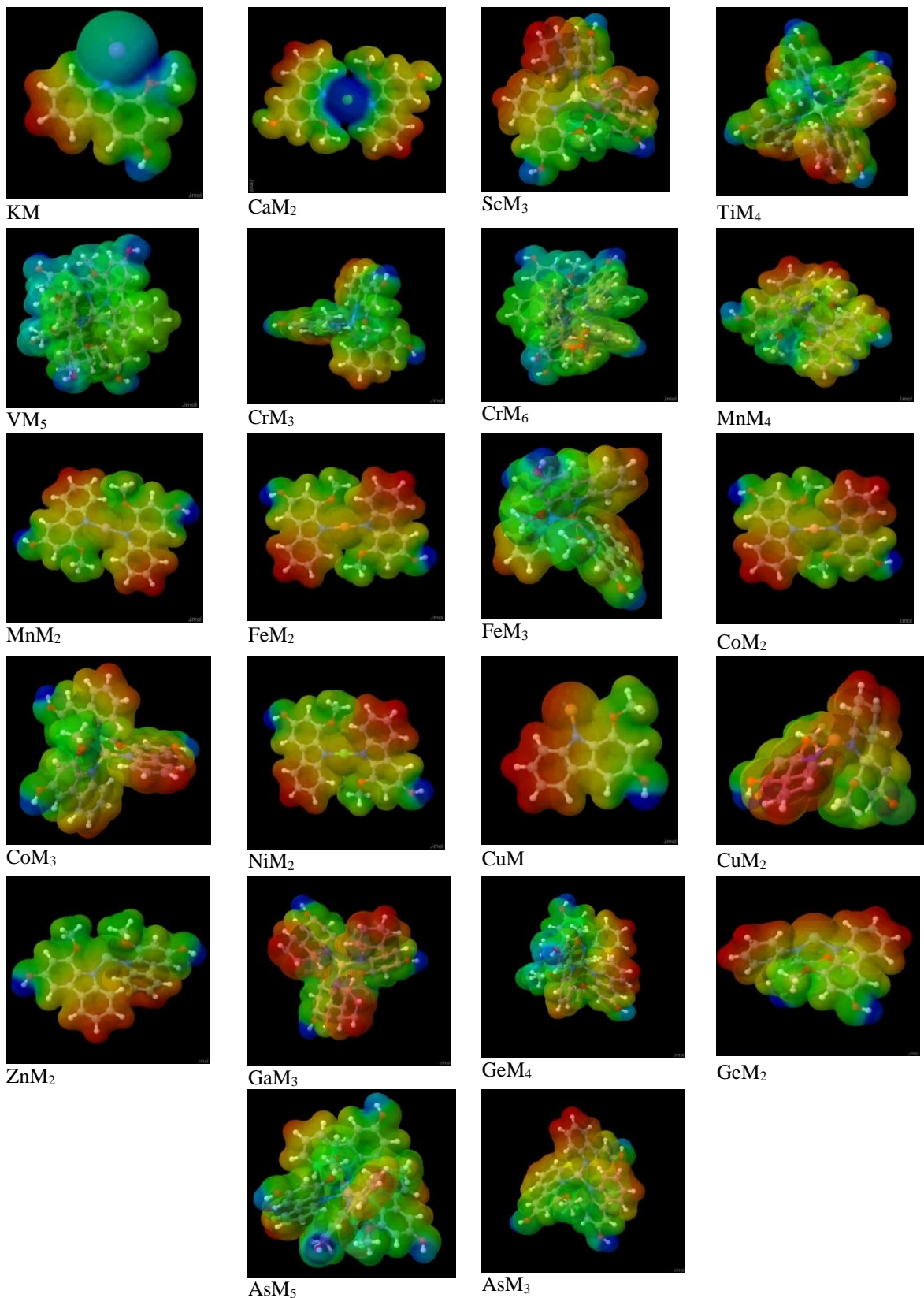
Figure 4. ESP visualization of murrastanine-a complexes

In the KM and CaM_2 complex compounds, there is no charge distribution, which is indicated in the center, a positive area is still formed which is marked in blue. This is because the electrostatic attraction with the central metal is not strong enough so that a less dense and less stable complex is formed [4]. Following the statement of Muthaiah, Bhatia and Kannan, 2020 that a higher oxidation state and smaller metal cation size can form more stable complexes [32]. This can be the cause of the formation of KM and CaM_2 complexes which are less stable, while the murrastanine-a complex with other metals can be stable.

CONCLUSIONS

Based on the results of the research that has been carried out, it can be concluded that by conjugating period 4 metals can reduce the energy gap of the murrastanine-a compound from 4.479 eV to 4.444 until 0.019 eV. A decrease in the energy gap occurs in all complexes with period 4 metals except for the metallic gallium.

The presence of conjugation with period 4 metals makes the energy gap of murrastanine-a diverse so that it can expand its potential use. Complexes VM_5, CrM_3, CrM_6, MnM_4, MnM_2, FeM_2, FeM_3, CoM_2, CoM_3, NiM_2, and CuM can potentially be used as infrared sensors or body temperature sensors. CaM_2, CuM_2, and AsM_5 complexes can be potential as high-temperature sensors. $CrM6$ and $FeM2$ complexes can be potential as solar cells. The KM, CaM_2, TiM_4, ZnM_2, GeM_2, and AsM_3 complexes can be potential as blue LED devices.

Based on the charge distribution of the murrastanine-a metal complex, it was shown that all period 4 metal complexes with murrastanine-a produced a stable complex, except for the KM and $CaM2$ complexes which were characterized by no charge distribution.

ACKNOWLEDGEMENTS

REFERENCES

1. Y. Oktaviani and Astuti, "Sintesis Lapisan Tipis Semikonduktor dengan Bahan Dasar Tembaga (Cu) Menggunakan Chemical Bath Deposition," *J. Fis. Unand*, vol. 3, no. 1, pp. 53–58, 2014.
2. K. W. Böer and U. W. Pohl, "The Origin of Band Structure," in *Semiconductor Physics*, Cham: Springer International Publishing, 2018, pp. 183–206.
3. P. Horley, P. J. G. Ribeiro, J. A. A. Martinez, and V. J. R. Vieira, "Semiconductor Fundamentals," in *Semiconductors Synthesis, Properties and Applications*, M. I. Pech-Canul and N. M. Ravindra, Eds. Cham: Springer International Publishing, 2019, pp. 1–36.
4. H. Wahyudah, "Kajian Teoritis Penentuan Kompleks Delfidin sebagai Bahan Dasar Fotosensor," Universitas Negeri Surabaya, 2016.
5. D. Prasad and V. Nath, "An Overview of Temperature Sensors," in *Proceeding of the Second International Conference on Microelectronics, Computing & Communication Systems (MCCS 2017)*, 2019, pp. 777–784.
6. N. Zhang, "4H-Silicon Carbide PN Diode for Harsh Environment Temperature Sensing Applications," Berkeley, 2014.
7. F. Zhuge *et al.*, "Nanostructured Materials and Architectures for Advanced Infrared Photodetection," *Adv. Mater. Technol.*, vol. 2, no. 8, p. 1700005, Aug. 2017.
8. S. Rühle, "Tabulated values of the Shockley–Queisser limit for single junction solar cells," *Sol. Energy*, vol. 130, pp. 139–147, Jun. 2016.
9. M. Freunek, M. Freunek, and L. M. Reindl, "Maximum efficiencies of indoor photovoltaic devices," *IEEE J. Photovoltaics*, vol. 3, no. 1, pp. 59–64, Jan. 2013.
10. G. Jarosz, R. Marczyński, and R. Signerski, "Effect of band gap on power conversion efficiency of single-junction semiconductor photovoltaic cells under white light phosphor-based LED illumination," *Mater. Sci. Semicond. Process.*, vol. 107, p. 104812, Mar. 2020.
11. T. Fang, F. Zhang, S. Yuan, H. Zeng, and J. Song, "Recent advances and prospects toward blue perovskite materials and light-emitting diodes," *InfoMat*, vol. 1, no. 2, pp. 211–233, Jun. 2019.

12. G. Pamungkas and I. G. M. Sanjaya, "Kajian Teoritis untuk Menentukan Celah Energi Porfirin Terkonjugasi Logam Kalsium Menggunakan Toeri Fungsional Kerapatan (DFT)," *Unesa J. Chem.*, vol. 2, no. 1, pp. 54–61, 2013.

13. K. Zhou and Y. Zhou, "Introduction to Organic-Inorganic Heterojunction," in *Optoelectronic Organic–Inorganic Semiconductor Heterojunctions*, Y. Zhou, Ed. London: CRC press, 2021, pp. 1–9.

14. S.-P. Tan, A. M. Ali, M. A. Nafiah, K. Awang, and K. Ahmad, "Isolation and cytotoxic investigation of new carbazole alkaloids from Murraya koenigii (Linn.) Spreng," *Tetrahedron*, vol. 71, no. 23, pp. 3946–3953, Jun. 2015.

15. K. Kubota, S. Hirata, Y. Shibano, O. Hirata, M. Yahiro, and C. Adachi, "Liquid Carbazole Substituted with a Poly(ethylene oxide) Group and Its Application for Liquid Organic Light-emitting Diodes," *Chem. Lett.*, vol. 41, no. 9, pp. 934–936, Sep. 2012.

16. F. A. Cotton and G. Wilkinson, *Advanced Inorganic Chemistry*, 5th ed. New York: John Wiley & Sons, 1988.

17. T. P. Hanusa, "Group 1s and 2s Metals," in *Comprehensive Coordination Chemistry II*, 2nd ed., J. A. McCleverty and T. J. Meyer, Eds. New York: Elsevier, 2003, pp. 1–92.

18. W. Levason and G. Reid, "Arsenic, Antimony, and Bismuth," in *Comprehensive Coordination Chemistry II*, 2nd ed., J. A. McCleverty and T. J. Meyer, Eds. New York: Elsevier, 2003, pp. 465–544.

19. J. Parr, "Germanium, Tin, and Lead," in *Comprehensive Coordination Chemistry II*, 2nd ed., J. A. McCleverty and T. J. Meyer, Eds. New York: Elsevier, 2003, pp. 545–608.

20. G. H. Robinson, "Aluminum and Gallium," in *Comprehensive Coordination Chemistry II*, 2nd ed., J. A. McCleverty and T. J. Meyer, Eds. New York: Elsevier, 2003, pp. 347–382.

21. K. Tanaka, "Electronic Structures of Organic Semiconductors," in *Organic Semiconductors for Optoelectronic*, 1st ed., H. Naito, Ed. Chichester: John Wiley & Sons, 2021, pp. 1–40.

22. F. Jensen, *Introduction to Computational Chemistry*, 3rd ed. Chichester: John Wiley & Sons, 2017.

23. R. A. Miranda and Quintana, "Density Functional Theory for Chemical Reactivity," in *Conceptual Density Functional Theory and Its Application in The Chemical Domain*, N. Islam and S. Kaya, Eds. Oakville: Apple Academic Press, 2018, pp. 15–44.

24. A. T. Apriliani, "Studi Komputasi Sifat Elektronik Senyawa Turunan Carbazole sebagai Sensitiser pada Dye-Sensitized Solar Cell (DSSC)," Institut Teknologi Sepuluh Nopember Surabaya, 2017.

25. J. Olsen, "An Introduction and Overview of Basis Sets for Molecular and Solid-State Calculations," in *Basis Sets in Computational Chemistry*, E. Perlt, Ed. irvine: Springer Nature Switzerland AG, 2020, pp. 1–16.

26. M. Valiev *et al.*, "NWChem: A comprehensive and scalable open-source solution for large scale molecular simulations," *Comput. Phys. Commun.*, vol. 181, no. 9, pp. 1477–1489, Sep. 2010.

27. A. Khorsand Zak, N. S. Abd Aziz, A. M. Hashim, and F. Kordi, "XPS and UV–vis studies of Ga-doped zinc oxide nanoparticles synthesized by gelatin based sol-gel approach," *Ceram. Int.*, vol. 42, no. 12, pp. 13605–13611, Sep. 2016.

28. N. Narayanan and D. NK, "Ga Dopant Induced Band Gap Broadening and Conductivity Enhancement in Spray Pyrolysed Zn0.85Ca0.15O thin Films," *Mater. Res.*, vol. 21, no. 6, pp. 1–7, Sep. 2018.

29. N. Rosyidah, "Sintesis Nanopartikel Zn1-xAlxO dengan Metode Kopresipitasi dan Karakterisasi Sifat Listrik," Institut Teknologi Sepuluh Nopember, 2016.

30. W. L. Masterton, C. N. Hurley, and E. J. Neth, *Chemistry: Principles, and Reactions*, 7th ed. Belmont: Brooks/Cole Cengage Learning, 2012.

31. O. A. Adegoke, "Chemical Derivatization Methodologies for UV-Visible Spectrophotometric Determination of Pharmaceuticals," *Int. J. Pharm. Sci. Rev. Res.*, vol. 14, no. 2, pp. 6–24, 2012.

32. S. Muthaiah, A. Bhatia, and M. Kannan, "Stability of Metal Complexes," in *Stability and Applications of Coordination Compounds*, A. Srivastva, Ed. London: IntechOpen, 2020.